International Journal of Impact Engineering 98 (2016) 88–96

Contents lists available at ScienceDirect

International Journal of Impact Engineering

journal homepage: www.elsevier.com/locate/ijimpeng

Review

Experimental study on external strong magnetic fields coupling with the shaped charge jet

Bin Ma, Zheng-xiang Huang *, Xu-dong Zu, Qiang-qiang Xiao

School of Mechanical Engineering, Nanjing University of Science and Technology, Nanjing 210094, PR China

ARTICLE INFO

Article history:
Received 11 December 2015
Received in revised form 6 August 2016
Accepted 18 August 2016
Available online 30 August 2016

Keywords:
Shaped charge jet
Magnetic field
Penetration
Stability

ABSTRACT

In this paper, the effect of an external magnetic field on a jet produced by a Ø 56 mm shaped charge was evaluated using the depth of penetration (DOP) test method. A standoff of 650 mm (11.61 CD) was used in the experiments. The shaped charge jet could undergo formation, elongation, breakup, rotation, and drift under this standoff. The initial energy was provided by a capacitor that was loaded into the solenoid to generate a magnetic field to couple with the jet. The initial voltage at both ends of the capacitors was 20.4 kV, and the discharge current of the circuit and magnetic induction intensity were analyzed. Experimental results indicated that a strong external magnetic field could enhance the stability of the jet and increase its DOP. The penetration ability of the jet is increased by 72.4% under the influence of the external magnetic field.

1. Introduction

Shaped charge jets (SCJs) are used extensively in many industries, including petroleum and defense applications, because of their significant penetration capability. SCJs show high penetration capability because of their high velocity; this ability is determined by their effective length and the density of the material used [1]. However, after a certain length of time (the breakup time), the jet becomes unstable and breaks up into many pieces approximately equal in size. Performance of the jet is significantly degraded when this occurs [2]. The penetration of a SCJ into most target materials increases to a maximum and subsequently decreases as the standoff distance increases [3]. In general, the maximum depth of penetration (DOP) occurs just prior to the onset of jet breakup because dispersion, spread, and tumbling of jet particles occur after breakup. The instability of SCJs is also an important factor responsible for this phenomenon. Therefore, the instability and breakup phenomena of SCJs have received a vast quantity of attention over the past few decades. Previous methods of increasing stability mainly focused on improving the physical–mechanical properties of SCJ materials and the machining process; the shape and size of liners have also been optimized. Unfortunately, stability problems of SCJs are not resolved perfectly through these traditional methods. Previous research has shown that the penetration capability of shaped charges can be controlled by electromagnetic actions [4]. If the development of plastic instability during stretching of SCJs could be decelerated under the influence of a magnetic field, it can increase their effective length. For the effect of a low-frequency magnetic field on SCJs, electromagnetic forces caused by electromagnetic induction are compressive during the diffusion stage of magnetic field into SCJ's material, and they are larger in the bulges zones; these forces become stretching during the elongation stage of SCJs, and their value is larger in the neck regions [5]. Electromagnetic induction occurs inside SCJs which are formed through explosive collapse of a metallic liner, when SCJs pass through a strong external magnetic field. Thus, the stability of a SCJ is expected to increase under the coupling effect of a magnetic field.

This finding has motivated studies on non-traditional approaches to increase the penetration of SCJs. In practice, magnetic fields are generated using an elongated solenoid placed on the path of jet propagation. Due to variations in time and space, and a reasonable relationship with time in an external magnetic field should be guaranteed to ensure the complete diffusion of the field into the SCJ material. Jet elements are stretched longer under the action of electromagnetic forces produced by a magnetic field coupled with the SCJ. Appropriate circuit parameters should be selected, and the SCJ elements passing through the solenoid are completely coupled with these fields. Fig. 1 shows the coupling between an SCJ and external magnetic field. Littlefield used linear perturbation theory to analyze the stability of rapidly stretching, and perfectly plastic jets when subjected to axial magnetic fields found that action of the fields inhibits the growth rates of instabilities in the jet [2]. Fedorov et al. showed that jet stretching with a diffused magnetic field is accompanied by magnetic field compression inside the jet, resulting in the appearance of radial stretching electromagnetic forces; in this study, the increase (10%) in DOP was observed when the magnetic field induction is changed from 1 Tesla to 10 Tesla. The authors then

* Corresponding author. School of Mechanical Engineering, Nanjing University of Science and Technology, Nanjing 210094, PR China. Fax: +86 025 84315454.
E-mail address: huangyu@mail.njust.edu.cn (Z. Huang).

http://dx.doi.org/10.1016/j.ijimpeng.2016.08.007
0734-743X/

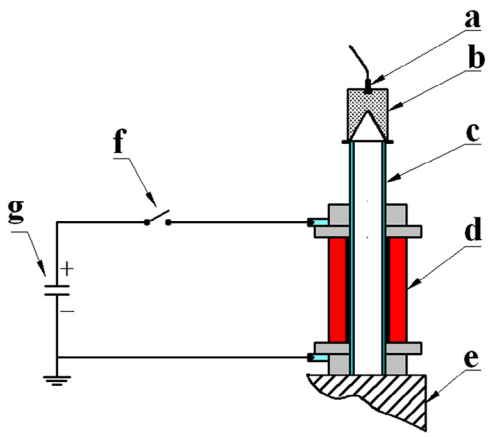

Fig. 1. Coupling between a shaped charge jet and external magnetic field. (a) Detonator, (b) Ø 56 mm Shaped Charge, (c) Standoff, (d) Solenoid, (e) Target, (f) Delay-action switch, (g) Capacitors.

introduced several kinds of electromagnetic actions controlling the jet at different stages of shaped charge firing and considered the salient deformation features of metal cumulative jets in a longitudinal low-frequency magnetic field on the basis of a model of a uniformly stretching cylindrical incompressible rigid-plastic conducting rod [1,6,7].

The stability mechanisms of the SCJ inside the magnetic field are very complex because of the interaction between the electromagnetic field and the SCJ. In addition, the available experimental data in the literature are limited. Hence, in the present study, experiments on the DOP of SCJs coupled with the external strong magnetic field are performed. The magnetic induction intensity is calculated as the jet elements pass through the solenoid, and the experimental results are compared with the results obtained without a magnetic field.

2. Characteristics of the circuit

2.1. Discharge current

The circuit structure is a typical RLC circuit. *R*, *L*, *C*, U_0, and *I(t)* are assumed to represent the resistance, induction, capacitance, voltage of capacitors at both ends, and circuital current, respectively. Thus, discharge current can be expressed as follows:

$$I(t)=\frac{U_0}{\omega L}e^{-\zeta t}\sin(\omega t) \tag{1}$$

where ξ=R/(2L) is the attenuation coefficient, and $\omega=\sqrt{\frac{1}{LC}-\left(\frac{R}{2L}\right)^2}$ is the oscillation frequency.

2.2. Electrical resistivity of conductors

The electrical resistivity of conductors is changed by the heating effect of the current. Hence, a current action integral model for conductor resistivity is applied [8]. This model uses the experimental values for copper based on exploding wire experiments [9]. The current action integral *J* could be expressed as follows:

$$J=\int_0^t j^2dt \tag{2}$$

where *j* represents the current density.

The resistivity model considers the different phases until wire explosion. Assuming that J_S and J_M are the values of the action integrals at the onset of melting and when the copper conductor is fully molten, respectively, and that ρ_S and ρ_M are the resistivities for the solid and molten phases at 1356 K, respectively, the resistivity for different phases can be obtained as follows:

$$\rho=\begin{cases}\rho_0 e^{\frac{J}{J_s}\ln\frac{\rho_s}{\rho_0}} & 0\le J\le J_s\\ \dfrac{\rho_s}{\sqrt{\dfrac{(J-J_s)(\rho_s^2-\rho_m^2)}{(J_m-J_s)\rho_m^2}+1}} & J_s\le J\le J_m\end{cases} \tag{3}$$

2.3. Evolution of the magnetic field

According to virtual origin theory, the virtual origin sets on the vertex of the liner, thus, the magnetic induction intensity on the axial region of a solenoid can be written as follows:

$$B(z_1)=\frac{\mu_0 j(t)}{2}\left[z_1\ln\left(\frac{R_2+\sqrt{R_2^2+z_1^2}}{R_1+\sqrt{R_1^2+z_1^2}}\right)-(z_1-2b)\ln\left(\frac{R_2+\sqrt{R_2^2+(z_1-b)^2}}{R_1+\sqrt{R_1^2+(z_1-b)^2}}\right)\right] \tag{4}$$

The moment of the closed circuit is the zero time, $z_1=z-(\Delta L+z_0)$ is the axial coordinate of the solenoid, *z* is the coordinate starting from the vertex of the liner, △L is the distance between the entrance of the solenoid and the virtual origin, and z_0 is the displacement coordinate of the virtual origin. In addition, *b*, R_1, and R_2 are the length, inner radius, and outer radius of the solenoid, respectively.

The average magnetic induction intensity when the element passes the solenoid can be obtained using the integral of the magnetic induction intensity on displacement. This intensity can be expressed as follows:

$$B=\frac{1}{z_f-z_s}\int_{z_s}^{z_f}B(z_1)dz_1 \tag{5}$$

where z_s is the element's starting position when the circuit is connected, z_f is the coordinate of exit of the solenoid, and z_1 is the current coordinate.

3. Experiments

3.1. The shaped charge used in the experiments

The diameter of the shaped charge used in experiments is 56 mm, and its length is 73 mm. The thickness of the conical copper liner is 0.8 mm, and the cone angle is 60°. In addition, the explosive used is JH-2 high explosive without a shell. Its total weight is 203 g (Fig. 2).

3.2. X-ray experiments

To obtain the jet parameters, X-ray experiments are carried out. X-ray images of the jet at 30 and 50 μs after detonation are obtained and shown in Fig. 3. According to the experimental results, the velocity of the jet tip and tail are 6.3 and 1.2 mm/μs, the diameters of the tip and tail 30 μs after detonation are 2 and 14 mm, and the lengths are 113 and 219 mm at 30 and 50 μs, respectively.

To better illustrate the performance of Ø 56 mm shaped charge, the DOPs of jets at different standoffs are theoretically calculated, and relevant experimental verifications are carried out. For each standoff, an average value of DOP is obtained through the experiments. The theoretical standoff curve and experimental results are shown in Fig. 4.